



**HAL**  
open science

## Combinatorial regulation of hepatic cytoplasmic signaling and nuclear transcriptional events by the OGT/REV-ERB $\alpha$ complex

Alexandre Berthier, Manjula Vinod, Geoffrey Porez, Agata Steenackers, Jérémy Alexandre, Nao Yamakawa, Céline Gheeraert, Maheul Ploton, Xavier Marechal, Julie Dubois-Chevalier, et al.

### ► To cite this version:

Alexandre Berthier, Manjula Vinod, Geoffrey Porez, Agata Steenackers, Jérémy Alexandre, et al.. Combinatorial regulation of hepatic cytoplasmic signaling and nuclear transcriptional events by the OGT/REV-ERB $\alpha$  complex. Proceedings of the National Academy of Sciences of the United States of America, 2018, 115 (47), pp.11033-11042. 10.1073/pnas.1805397115 . inserm-01924835

**HAL Id: inserm-01924835**

**<https://inserm.hal.science/inserm-01924835>**

Submitted on 16 Nov 2018

**HAL** is a multi-disciplinary open access archive for the deposit and dissemination of scientific research documents, whether they are published or not. The documents may come from teaching and research institutions in France or abroad, or from public or private research centers.

L'archive ouverte pluridisciplinaire **HAL**, est destinée au dépôt et à la diffusion de documents scientifiques de niveau recherche, publiés ou non, émanant des établissements d'enseignement et de recherche français ou étrangers, des laboratoires publics ou privés.



# Combinatorial regulation of hepatic cytoplasmic signaling and nuclear transcriptional events by the OGT/REV-ERB $\alpha$ complex

Alexandre Berthier<sup>a</sup>, Manjula Vinod<sup>a</sup>, Geoffrey Porez<sup>a</sup>, Agata Steenackers<sup>b</sup>, Jérémy Alexandre<sup>a</sup>, Nao Yamakawa<sup>b</sup>, Céline Gheeraert<sup>a</sup>, Maheul Ploton<sup>a</sup>, Xavier Maréchal<sup>a</sup>, Julie Dubois-Chevalier<sup>a</sup>, Agnès Hovasse<sup>c</sup>, Christine Schaeffer-Reiss<sup>c</sup>, Sarah Cianféroni<sup>c</sup>, Christian Rolando<sup>d,e,f</sup>, Fabrice Bray<sup>d,e,f</sup>, Hélène Duez<sup>a</sup>, Jérôme Eeckhoutte<sup>a</sup>, Tony Lefebvre<sup>b</sup>, Bart Staels<sup>a</sup>, and Philippe Lefebvre<sup>a,1</sup>

<sup>a</sup>University of Lille, Inserm, Centre Hospitalier Universitaire de Lille, Institut Pasteur de Lille, European Genomic Institute for Diabetes, U1011, Lille F-59045, France; <sup>b</sup>University of Lille, CNRS, Unité de Glycobiologie Structurale et Fonctionnelle, UMR 8576, Villeneuve d'Ascq F-59655, France; <sup>c</sup>Laboratoire de Spectrométrie de Masse BioOrganique, University of Strasbourg, CNRS, Institut Pluridisciplinaire Hubert Curien, UMR 7178, Strasbourg F-67037, France; <sup>d</sup>Miniaturisation pour la Synthèse, l'Analyse & la Protéomique, CNRS, Unité de Service et de Recherche (USR) 3290, University of Lille, Villeneuve d'Ascq F-59655, France; <sup>e</sup>Fédération de Recherche Biochimie Structurale et Fonctionnelle des Assemblages Biomoléculaires FRABio, FR 3688 CNRS, University of Lille, Villeneuve d'Ascq F-59655, France; and <sup>f</sup>Institut M.-E. Chevreul, CNRS, FR 2638, University of Lille, Villeneuve d'Ascq F-59655, France

Edited by Steven A. Kliewer, The University of Texas Southwestern Medical Center, Dallas, TX, and approved October 10, 2018 (received for review March 28, 2018)

The nuclear receptor REV-ERB $\alpha$  integrates the circadian clock with hepatic glucose and lipid metabolism by nucleating transcriptional comodulators at genomic regulatory regions. An interactomic approach identified O-GlcNAc transferase (OGT) as a REV-ERB $\alpha$ -interacting protein. By shielding cytoplasmic OGT from proteasomal degradation and favoring OGT activity in the nucleus, REV-ERB $\alpha$  cyclically increased O-GlcNAcylation of multiple cytoplasmic and nuclear proteins as a function of its rhythmically regulated expression, while REV-ERB $\alpha$  ligands mostly affected cytoplasmic OGT activity. We illustrate this finding by showing that REV-ERB $\alpha$  controls OGT-dependent activities of the cytoplasmic protein kinase AKT, an essential relay in insulin signaling, and of ten-of-eleven translocation (TET) enzymes in the nucleus. AKT phosphorylation was inversely correlated to REV-ERB $\alpha$  expression. REV-ERB $\alpha$  enhanced TET activity and DNA hydroxymethylated cytosine (5hmC) levels in the vicinity of REV-ERB $\alpha$  genomic binding sites. As an example, we show that the REV-ERB $\alpha$ /OGT complex modulates *SREBP-1c* gene expression throughout the fasting/feeding periods by first repressing AKT phosphorylation and by epigenomically priming the *Srebf1* promoter for a further rapid response to insulin. Conclusion: REV-ERB $\alpha$  regulates cytoplasmic and nuclear OGT-controlled processes that integrate at the hepatic *SREBF1* locus to control basal and insulin-induced expression of the temporally and nutritionally regulated lipogenic *SREBP-1c* transcript.

O-GlcNAcylation | REV-ERB $\alpha$  | metabolism | epigenomics | signal transduction

O-GlcNAcylation is a posttranslational modification (PTM) targeting both cytoplasmic and nuclear proteins (1), affecting their cellular sublocalization, stability, and/or activity (2). O-GlcNAcylation involves a biosynthetic arm, the hexosamine biosynthetic pathway (HBP), and a catalytic arm acting through two enzymes with opposite activities, namely O-GlcNAc transferase (OGT) catalyzing *N*-acetylglucosamine (GlcNAc) transfer from UDP-GlcNAc to polypeptides, and O-GlcNAcase (OGA/MGEA5), which removes this sugar moiety (3). As generation of the rate-limiting UDP-GlcNAc requires glucose (Glc), glutamine, gluconeogenic or ketogenic amino acids, fatty acids, uridine, and ATP as precursors, OGT activity reflects the cellular metabolic status (2). OGT modifies hundreds of proteins, including proteins involved in the regulation of metabolism, such as carbohydrate-responsive element-binding protein (ChREBP) (4). OGT also couples metabolism to epigenomic control of transcription. As an example, when integrated into a host cell factor 1 (HCF-1)/OGT complex, PGC1 $\alpha$  is O-GlcNAcylation and

is protected from ubiquitylation and degradation (5). In addition, OGT interacts with the corepressor Sin3a and ten-eleven translocation (TET methylcytosine hydroxylases) family members to O-GlcNAcylation RNA polymerase II and histone H2B (6). Hence, OGT imposes a metabolic control over transcriptional regulation.

The cyclically expressed nuclear receptors REV-ERB $\alpha$  and REV-ERB $\beta$  are key transcription factors involved in the regulation of the circadian clock machinery and of metabolism. Genetic ablation of *Rev-erb $\alpha$*  and/or *Rev-erb $\beta$*  influences adipocyte differentiation, lipid, cholesterol, and glucose metabolism and leads to cardiometabolic abnormalities (7). REV-ERB $\alpha$  has a prominent regulatory role in hepatic metabolism by acting as a transcriptional repressor regulated by small synthetic ligands and heme, its natural ligand (8). REV-ERB $\alpha$  represses gene expression by recruiting a HDAC3/NCoR corepressor complex in a ligand-dependent manner, and liver *Hdac3* or *Ncor* gene deletion partially phenocopies that of *Rev-erb $\alpha$*  (9, 10). Recent data suggest that REV-ERB $\alpha$  regulates liver metabolic gene expression through tethering to HNF6, whereas clock genes are regulated through direct DNA binding (11). REV-ERB $\alpha$ , through its interaction with HSP90, affects the stability of the glucocorticoid

## Significance

Using an interactomic approach, we have identified the nuclear receptor REV-ERB $\alpha$  as a O-GlcNAc transferase (OGT) protein partner. REV-ERB $\alpha$  protects cytoplasmic OGT from proteasomal degradation and facilitates cytosolic and nuclear protein O-GlcNAcylation while REV-ER $\alpha$  ligands decreased cytoplasmic OGT activity. REV-ERB $\alpha$  thus exerts pleiotropic activities through OGT, coordinating signal transduction, epigenomic programming, and transcriptional response in the liver.

Author contributions: A.B., G.P., A.S., N.Y., C.S.-R., S.C., C.R., J.E., T.L., and P.L. designed research; A.B., M.V., G.P., A.S., J.A., N.Y., C.G., M.P., X.M., J.D.-C., A.H., C.S.-R., F.B., H.D., J.E., and T.L. performed research; M.V., A.S., J.A., N.Y., C.G., M.P., X.M., J.D.-C., A.H., C.S.-R., S.C., C.R., F.B., H.D., T.L., and P.L. contributed new reagents/analytic tools; A.B., M.V., G.P., A.S., N.Y., C.G., J.D.-C., C.S.-R., S.C., F.B., J.E., T.L., B.S., and P.L. analyzed data; and J.E., T.L., B.S., and P.L. wrote the paper.

The authors declare no conflict of interest.

This article is a PNAS Direct Submission.

This open access article is distributed under Creative Commons Attribution-NonCommercial-NoDerivatives License 4.0 (CC BY-NC-ND).

<sup>1</sup>To whom correspondence should be addressed. Email: philippe-claude.lefebvre@inserm.fr.

This article contains supporting information online at [www.pnas.org/lookup/suppl/doi:10.1073/pnas.1805397115/-DCSupplemental](http://www.pnas.org/lookup/suppl/doi:10.1073/pnas.1805397115/-DCSupplemental).

receptor (12). REV-ERB $\alpha$  thus increases its functional versatility by engaging in various protein–protein interactions. However, little is known about other REV-ERB $\alpha$  interaction partners and associated functions. In this study, we have identified OGT as a binding partner of REV-ERB $\alpha$ , and we have characterized the functional consequences of this partnership on integrated hepatic intracellular signaling.

## Results

**REV-ERB $\alpha$  Interacts with OGT.** To identify novel REV-ERB $\alpha$ –interacting proteins, nuclear extracts from human hepatoma HepG2 cells were cross-linked then immunoprecipitated using a REV-ERB $\alpha$ –specific antibody. This procedure followed by nano LC-MS/MS (RIME; ref. 13) identified several nuclear REV-ERB $\alpha$ –interacting proteins (Fig. 1A, *Upper* and *SI Appendix, Table S1*), including the known REV-ERB $\alpha$  corepressor complex NCOR1/HDAC3 as well as OGT. The REV-ERB $\alpha$ /OGT interaction was confirmed by co-IP of native protein complexes (Fig. 1A, *Lower*). Considering the instrumental roles of both

proteins in controlling liver metabolism, we investigated the functional role(s) of the REV-ERB $\alpha$ /OGT interaction.

**REV-ERB $\alpha$  Regulates Cellular O-GlcNAcylation Levels.** We first monitored protein O-GlcNAcylation levels in HepG2 cells by Western blotting (WB) with an anti-O-GlcNAc antibody (RL2; Fig. 1B) at 25 mM Glc, a condition increasing protein O-GlcNAcylation (*SI Appendix, Fig. S1A*). siRNA-mediated knockdown of REV-ERB $\alpha$  or of OGT equally decreased protein O-GlcNAcylation and OGT levels (Fig. 1B). As REV-ERB $\alpha$  knockdown did not affect OGT mRNA expression (*SI Appendix, Fig. S1B*), we concluded that the REV-ERB $\alpha$  protein level controls OGT protein stability. REV-ERB $\alpha$  protein expression fluctuates in a circadian manner in mouse liver reaching the highest expression at ZT6–ZT12 (Fig. 1C and *SI Appendix, Fig. S1C*). Since REV-ERB $\alpha$  also interacts with OGT in liver extracts (*SI Appendix, Fig. S1D*), we examined whether O-GlcNAcylation regulation by REV-ERB $\alpha$  occurs in vivo. Protein O-GlcNAcylation was compared at ZT6 in wild-type and Rev-erb $\alpha$ –deficient mice. Protein O-GlcNAcylation and OGT protein expression were drastically reduced in Rev-erb $\alpha$ <sup>−/−</sup> livers

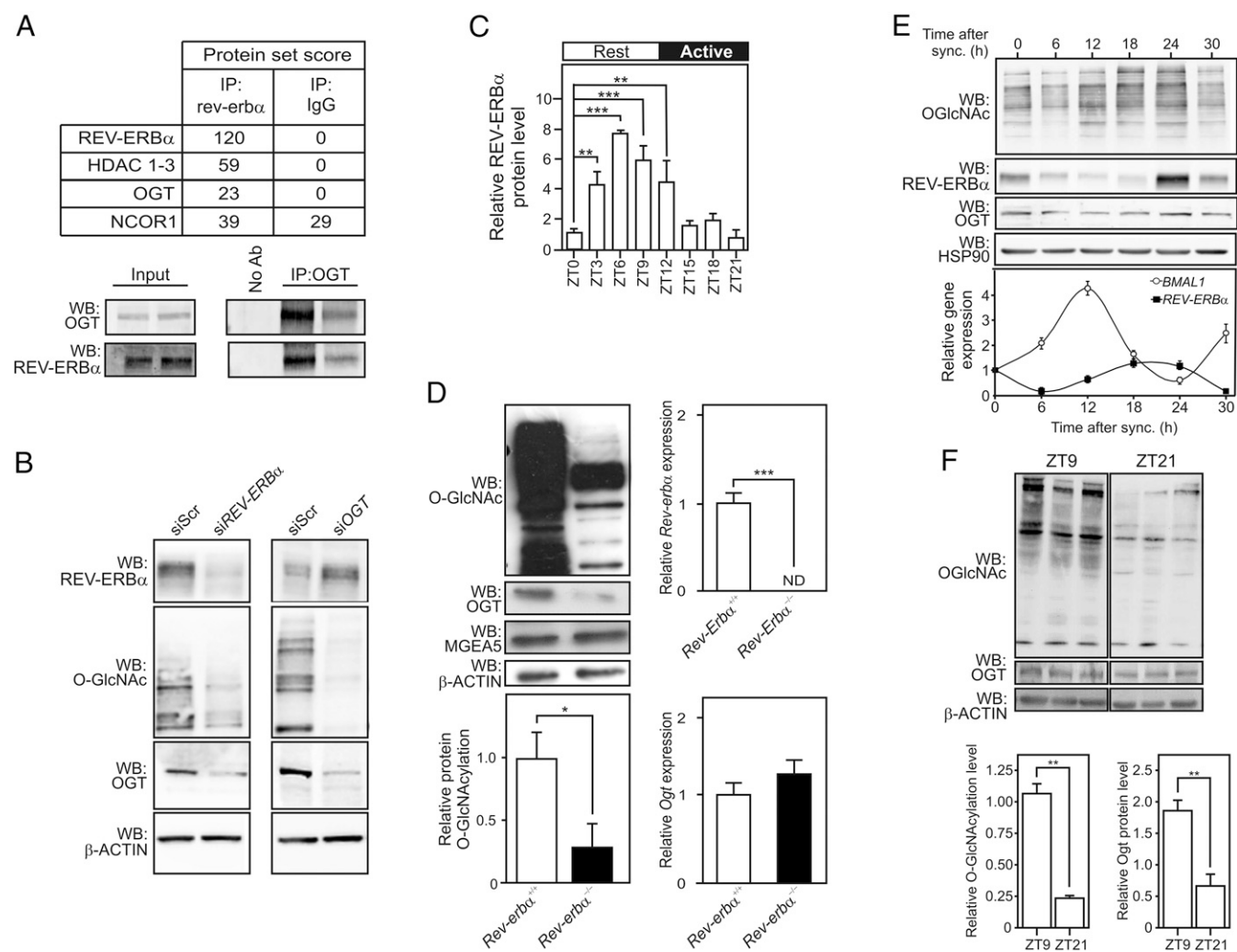


**Fig. 1.** REV-ERB $\alpha$  interacts with OGT and controls O-GlcNAcylation. (A) Most-relevant proteins identified by RIME in HepG2 cells extract (*Upper*). Validation of the REV-ERB $\alpha$ /OGT interaction by anti-OGT coimmunoprecipitation (IP) of HepG2 whole cellular extract followed by anti-OGT and anti-REV-ERB $\alpha$  WB ( $n = 2$ ; *Lower*). (B) O-GlcNAcylation levels in cellular extracts from HepG2 cells depleted from REV-ERB $\alpha$  or OGT mRNAs. (C) Time-dependent REV-ERB $\alpha$  protein expression level in mouse livers. (D) O-GlcNAcylation, OGT, and OGA protein levels in protein extracts from WT or Rev-erb $\alpha$ <sup>−/−</sup> mouse livers at ZT6. Rev-erb $\alpha$  and Ogt mRNA levels were assessed by RT-qPCR. ND, not detectable. (E) O-GlcNAcylation, REV-ERB $\alpha$ , and OGT protein levels (*Upper*) and REV-ERB $\alpha$  and BMAL1 relative gene expression (*Lower*) in synchronized U2OS cells. (F) O-GlcNAcylation and OGT protein levels in mouse livers at ZT9 and ZT21. Results are expressed as mean  $\pm$  SEM, and values were compared by a two-way ANOVA followed by a Bonferroni post hoc test (C) or a *t* test (D and F). \* $P < 0.05$ , \*\* $P < 0.01$ , \*\*\* $P < 0.001$ .



(Fig. 1D and *SI Appendix, Fig. S1E*), whereas *Ogt* mRNA steady-state levels were not altered in this genetic background (Fig. 1D).

*REV-ERB $\alpha$*  mRNA and protein expression cycles in synchronized human osteosarcoma U2OS cells. Maximal expression of *REV-ERB $\alpha$*  protein was observed in serum-shocked U2OS cells 24 h after synchronization and inversely correlated with *Bmal1* expression, a cognate direct *REV-ERB $\alpha$*  target gene (Fig. 1E). OGT and protein O-GlcNAcylation levels peaked 24 h after synchronization, thus following *REV-ERB $\alpha$*  protein expression and activity as monitored by Western blot and *BMAL1* expression, respectively, and exhibited a trough 30 h after the serum shock, corresponding to the nadir of *REV-ERB $\alpha$*  expression (Fig. 1E). Of note, OGT and O-GlcNAcylation fluctuations were not observed in an U2OS cell subclone in which *REV-ERB $\alpha$*  protein expression was abrogated through CrispR/Cas9-mediated gene inactivation (*SI Appendix, Fig. S1F, Left* and *SI Appendix, Fig. S1G*). Increased *REV-ERB $\alpha$* , OGT, and protein O-GlcNAcylation levels were also detected in mouse livers at ZT7 compared with ZT21, corresponding to maximal and minimal liver *REV-ERB $\alpha$*  protein expression in vivo, respectively (Fig. 1C and F). Taken together, these data show that the *REV-ERB $\alpha$*  protein level controls OGT protein level and/or activity. As *REV-ERB $\beta$*  displays overlapping functions with *REV-ERB $\alpha$*  (7, 9), we assessed whether *REV-ERB $\beta$*  also regulates protein O-GlcNAcylation in HepG2 cells. Knockdown of *REV-ERB $\beta$*  expression affected neither OGT expression nor cellular protein O-GlcNAcylation levels (*SI Appendix, Fig. S1A and B*). Furthermore, CrispR/Cas9-mediated *REV-ERB $\beta$*  gene ablation did not affect the circadian modulation of OGT and O-GlcNAcylation. (*SI Appendix, Fig. S1F, Right* and *SI Appendix, Fig. S1G*), showing that the observed OGT protein stabilization is *REV-ERB $\alpha$* -specific.

Whether a reciprocal regulation occurs between *REV-ERB $\alpha$*  and OGT was assessed (*SI Appendix, Fig. S2*). 6-diazo-5-oxo-1-norleucine (DON) is a chemical inhibitor of glucosamine-fructose-6-phosphate aminotransferase, which alters UDP-GlcNAc-dependent pathways including OGT-catalyzed O-GlcNAcylation. DON efficiently blunted the glucose-induced expression of liver pyruvate kinase known to be an OGT-dependent, ChREBP-mediated process (4). In contrast, glucose and/or DON treatments did not modify endogenous *REV-ERB $\alpha$*  transcriptional activity (*SI Appendix, Fig. S2A*) despite an observed stabilization of the *REV-ERB $\alpha$*  protein by DON. The ability of *REV-ERB $\alpha$*  to recruit the transcriptional corepressor NCOR1, as assessed in a mammalian two-hybrid assay, was neither altered by the OGA/MGEA5-specific inhibitor Thiamet G nor by the OGT activator glucosamine (*SI Appendix, Fig. S2B*). Immunoprecipitated *REV-ERB $\alpha$*  submitted to Click-it chemistry, which substitutes O-GlcNAc moieties with azido-modified galactose and allows subsequent detection with alkyne-derived markers, did not provide evidence for *REV-ERB $\alpha$*  O-GlcNAcylation (*SI Appendix, Fig. S2C*). The absence of *REV-ERB $\alpha$*  O-GlcNAcylation was confirmed by mass spectrometry analysis of *REV-ERB $\alpha$*  immunopurified from HepG2 cells. Therefore, *REV-ERB $\alpha$*  transcriptional activity is not sensitive to HBP modulation and *REV-ERB $\alpha$*  is not detectably O-GlcNAcyated in the studied conditions.

***REV-ERB $\alpha$*  Ligand Binding Interferes with O-GlcNAcylation.** We next assessed whether ligand binding to *REV-ERB $\alpha$*  affects protein O-GlcNAcylation. We first interfered with intracellular heme levels (typically around 2–4  $\mu$ M, ref. 14) in HepG2 cells by knocking down the expression of the rate-limiting heme synthesis enzyme ALAS1 (*SI Appendix, Fig. S3A*). This resulted in a modest but detectable decrease in heme level (*SI Appendix, Fig. S3B*) and in increased cellular protein O-GlcNAcylation (*SI Appendix, Fig. S3C*). This result was consistent with the effect of succinylacetone, a potent inhibitor of heme synthesis, which also increased protein O-GlcNAcylation at both low and high glucose concentrations without significantly altering *REV-ERB $\alpha$*  protein

levels (*SI Appendix, Fig. S3D*). As treatment of HepG2 cells with the heme precursor delta-aminolevulinic acid did not reproducibly induce major changes in protein O-GlcNAcylation probably due to an precise regulation of intracellular heme level (*SI Appendix, Fig. S3D*), we treated cells with the high affinity, heme-mimicking *REV-ERB $\alpha$*  synthetic agonist GSK4112 (Fig. 2A). This compound efficiently blunted protein O-GlcNAcylation at low and high glucose concentrations, again irrespectively of *REV-ERB $\alpha$*  protein levels (Fig. 2A). To ensure that this effect was mediated by *REV-ERB $\alpha$*  ligation, we compared the ability of wild-type *REV-ERB $\alpha$*  to regulate cellular protein O-GlcNAcylation to that of a heme binding-crippled *REV-ERB $\alpha$*  mutant. Heme binding to *REV-ERB $\alpha$*  ( $K_d$  2–4  $\mu$ M, ref. 15) is prevented by mutating H602 into F (16). *REV-ERB $\alpha$*  H602F displayed a decreased transcriptional repressive activity (Fig. 2B) when overexpressed in *REV-ERB $\alpha$* -negative HEK293 cells (*SI Appendix, Fig. S3E*). Treatment with the *REV-ERB* agonist GSK4112 blunted protein O-GlcNAcylation in the presence of wild-type *REV-ERB $\alpha$* -expressing cells, but not in H602F-expressing cells (Fig. 2C). Thus, *REV-ERB $\alpha$*  ligation decreases protein O-GlcNAcylation without affecting OGT level as opposed to *REV-ERB $\alpha$*  deficiency. Taken together, this suggests that *REV-ERB $\alpha$*  controls both OGT activity and activity.

***REV-ERB $\alpha$*  Modulates OGT Activity in both Cytoplasmic and Nuclear Compartments.** As we confirmed that OGT and *REV-ERB $\alpha$*  are located in both the cytoplasmic and nuclear compartments (refs. 2 and 17, Fig. 3A and B, and *SI Appendix, Fig. S4A*), thus possibly undergoing distinct cellular fates, we investigated the possibility that cytoplasmic and nuclear OGT could be regulated differentially by *REV-ERB $\alpha$* . We observed that OGT degradation, hence decreased total protein O-GlcNAcylation, triggered by *REV-ERB $\alpha$*  protein depletion was prevented upon 26S proteasome complex inhibition by MG132 (carbobenzoxy-Leu-Leu-leucinal) (*SI Appendix, Fig. S4B*). In contrast, the ligand-induced decrease in cellular protein O-GlcNAcylation was not MG132-sensitive (*SI Appendix, Fig. S4C*). Cell fractionation showed that *REV-ERB $\alpha$*  protein level decreased in the cytoplasm and increased in the nuclear compartment upon ligand treatment (Fig. 3B, *Upper* and *SI Appendix, Fig. S4A*), in agreement with a previous study (18). We thus tested the possibility that the altered *REV-ERB $\alpha$*  subcellular distribution triggered by GSK4112 selectively modifies OGT activity in the cytoplasmic and nucleoplasmic compartments (Fig. 3B). GSK4112 treatment blunted the glucose-induced O-GlcNAcylation of cytoplasmic proteins. In contrast, O-GlcNAcylation of nucleoplasmic proteins increased in these conditions, thus concomitant with ligand-induced nuclear accumulation of *REV-ERB $\alpha$*  and with increased interaction of nuclear OGT with *REV-ERB $\alpha$* . Proteasome inhibition prevented ligand-induced cytoplasmic *REV-ERB $\alpha$*  depletion and abolished the ligand-induced decrease of cytoplasmic *REV-ERB $\alpha$* /OGT interaction and O-GlcNAcylation levels (Fig. 3B). However, MG132 did not influence protein O-GlcNAcylation in the nuclear compartment, indicating that nuclear OGT is insensitive to proteasomal degradation (Fig. 3B). Taken together, these data suggest that ligand treatment triggers *REV-ERB $\alpha$*  cytoplasmic depletion, hence negatively impacting protein O-GlcNAcylation in a proteasome-dependent manner, while promoting its accumulation in the nucleus and interaction with OGT, hence increasing nuclear OGT activity.

***REV-ERB $\alpha$* -Dependent O-GlcNAcylation Targets Cytoplasmic and Nuclear Structural and Effector Proteins.** Since data above point at *REV-ERB $\alpha$*  protein expression and subcellular localization as a set point of protein O-GlcNAcylation, we identified cellular proteins whose O-GlcNAcylation is potentially controlled by *REV-ERB $\alpha$*  by label-free mass spectrometry. HepG2 cellular

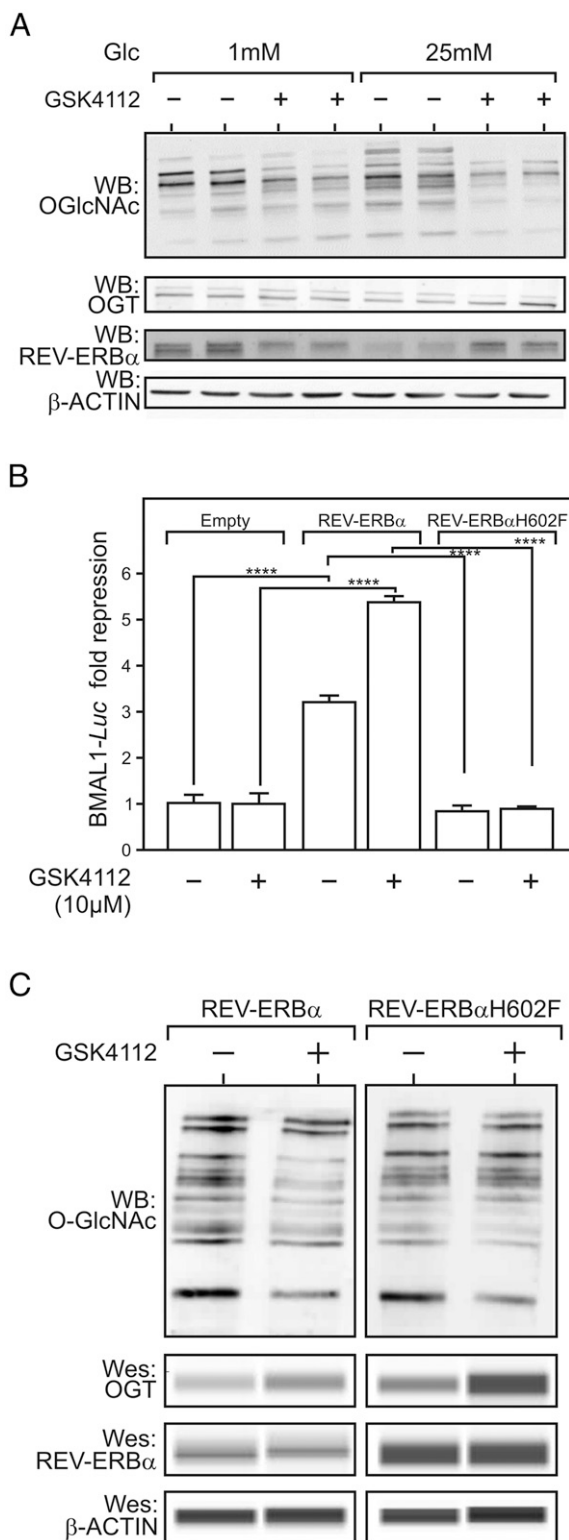


**Fig. 2.** REV-ERB $\alpha$  agonists reduce protein O-GlcNAcylation. (A) Protein O-GlcNAcylation, OGT, and REV-ERB $\alpha$  levels after treatment of HepG2 cells with the synthetic REV-ERB $\alpha$  agonist GSK4112 (10  $\mu$ M). (B) REV-ERB $\alpha$  repressive activity determined by a transactivation assay using a Bmal-luc reporter gene, expression vectors coding for either wild-type or mutated REV-ERB $\alpha$  (WT, H602F) or empty vector (empty) transfected into HEK293 cells treated or not with 10  $\mu$ M GSK4112. (C) O-GlcNAcylation, OGT, and REV-ERB $\alpha$  protein levels in HEK293 whole-cell extracts after transfection with REV-ERB $\alpha$  WT or H602F and treatment or not with 10  $\mu$ M GSK4112 at 25 mM Glc. Results are expressed as mean  $\pm$  SEM, and values were compared by a

extracts were immunoprecipitated with either a nonspecific IgG (Ctrl IgG) or the anti-O-GlcNAc antibody RL2, after transfection with a negative control siRNA (Ctrl) or an anti-REV-ERB $\alpha$  siRNA (Fig. 4A). This approach identified 281 proteins present in at least one condition, among which 71 were specifically enriched upon RL2 IP. Twenty-eight proteins were less represented in immunoprecipitates from REV-ERB $\alpha$ -depleted cells (Fig. 4A), including several previously identified O-GlcNAcylated proteins with structural, signaling, or transcriptional functions such as histone H2B, the transcription factors SP1 and SP3, HCFC1/VP16-accessory protein, and the protein kinase WNK1 (17, 19, 20). To detect lower expressed putative OGT targets, immunoprecipitates were also resolved by SDS/PAGE and areas of the gel ranging from 50 kDa to 170–200 kDa were analyzed by LC-MS/MS after tryptic digestion (Fig. 4B and *SI Appendix, Table S2*). Top ranking proteins again included HCFC1 and SP3, and interestingly other proteins such as OGT itself, the nuclear receptor coactivator CARM1, and AKT1. Although this approach could also potentially identify proteins with a decreased steady-state level in REV-ERB $\alpha$ -depleted cells or interacting with O-GlcNAcylated proteins, many of them have previously been described as bona fide OGT targets and O-GlcNAcylated polypeptides (17, 21, 22). As an example, both AKT and H2B were similarly expressed in naive and REV-ERB $\alpha$ -depleted cells, suggesting that OGT activity does not affect their stability (Fig. 4C). Taken together, these analyses show that REV-ERB $\alpha$  expression likely regulates the O-GlcNAcylation level of multiple cytoplasmic and nuclear proteins or of associated proteins with important regulatory functions (*SI Appendix, Table S2*).

**Cytoplasmic OGT Regulates AKT Phosphorylation in a REV-ERB $\alpha$ -Dependent Manner.** In response to insulin, AKT T308 and S473 are phosphorylated by PDK1 and mTORC2, respectively (23). O-GlcNAcylation impairs AKT phosphorylation and inhibits insulin signaling in mouse liver (22, 24). Since REV-ERB $\alpha$  overexpression increased AKT O-GlcNAcylation in HepG2 cells as assessed by Click-It chemistry (*SI Appendix, Fig. S5A*), we further tested whether REV-ERB $\alpha$  controls AKT phosphorylation. Overexpression of REV-ERB $\alpha$  through adenoviral transduction (Fig. 5A and *SI Appendix, Fig. S5 B and C*) increased OGT protein level and cellular protein O-GlcNAcylation levels (*SI Appendix, Fig. S5B*). In parallel, insulin-stimulated AKT phosphorylation decreased at both S473 and T308 upon REV-ERB $\alpha$  overexpression (Fig. 5A and *SI Appendix, Fig. S5C*). Conversely, REV-ERB $\alpha$  knockdown increased AKT phosphorylation (Fig. 5B and *SI Appendix, Fig. S5D*). To assess whether REV-ERB $\alpha$ -dependent OGT stabilization also controls AKT phosphorylation in vivo, OGT protein and AKT phosphorylation levels were analyzed in liver extracts from ad libitum-fed *Rev-erba*<sup>+/+</sup> or *Rev-erba*<sup>-/-</sup> mice. *Rev-erba* deficiency reduced OGT protein levels in mouse liver (Fig. 5C and *SI Appendix, Fig. S5E*) as described above (Fig. 1E). Both circadianly (ZT0) and genetically induced *Rev-erba* depletion (*Rev-erba*<sup>-/-</sup>) were associated with increased AKT T308 phosphorylation, which correlated with OGT protein levels (Fig. 5C and *SI Appendix, Fig. S5E*). The expression of the lipogenic transcription factor *Srebp1c* in mice is positively (auto)regulated through the insulin/AKT pathway and, after S1P/S2P-mediated processing, controls the expression of genes coding for lipid biosynthetic enzymes such as *Scd* and *Fasn* (25). Basal AKT phosphorylation at S473, a process known to be insulin-dependent (26), was significantly higher in fasted *Rev-erba*<sup>-/-</sup> liver, and T308 phosphorylation showed a similar trend. Similarly, phosphorylation levels were higher in refed *Rev-erba*<sup>-/-</sup> liver (Fig. 5D). In *Rev-erba*<sup>-/-</sup> mouse liver, the response to refeeding also translated into increased

two-way ANOVA followed by a Tukey post hoc test, \*\*\*\**P* < 0.0001. Wes, Simple Western (ProteinSimple).



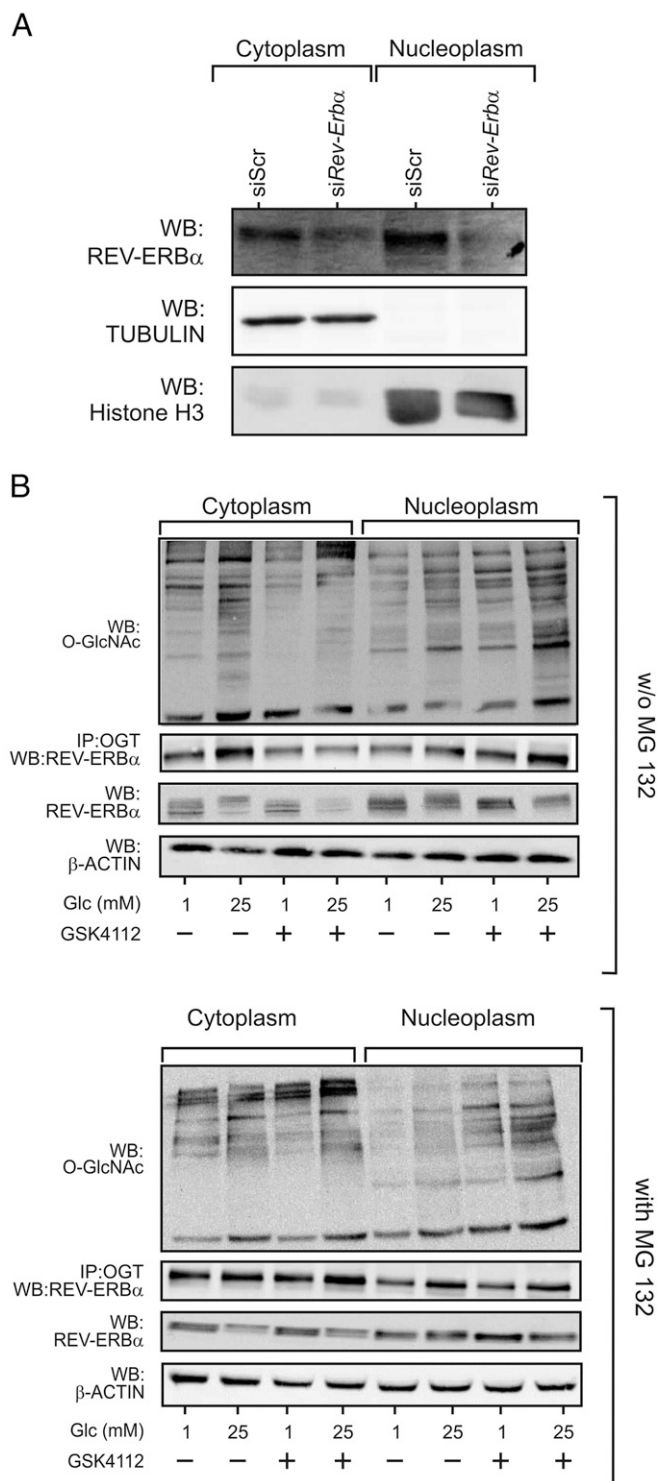


**Fig. 3.** REV-ERB $\alpha$  interaction with cytoplasmic OGT prevents its proteasomal degradation. (A) REV-ERB $\alpha$  is detected in both the cytoplasm and nucleus of target cells. Cytoplasmic and nuclear fractions from HepG2 cells were analyzed by WB for their REV-ERB $\alpha$  content. (B) Cytoplasmic and nuclear protein O-GlcNAcylation and REV-ERB $\alpha$  protein levels were determined by WB. The REV-ERB $\alpha$ /OGT interaction was analyzed by OGT IP followed by REV-ERB $\alpha$  WB analysis. HepG2 cells were cultured at 1 or 25 mM Glc and treated with 10  $\mu$ M GSK4112 with (Lower) or without (Upper) 5  $\mu$ M MG132.

hepatic expression of *Srebp1c* and of its target gene *Fasn* when compared its *Rev-erba*<sup>+/+</sup> counterpart (Fig. 5E). These findings

thus suggest that REV-ERB $\alpha$  also acts nontranscriptionally on this signaling axis by controlling AKT O-GlcNAcylation.

**TET Activity and Methylcytosine Hydroxylation Are REV-ERB $\alpha$ -Dependent.** The label-free mass spectroscopy analysis also identified H2B as a REV-ERB $\alpha$ -dependent O-GlcNAcylated protein (Fig. 4). Histone H2B O-GlcNAcylation is catalyzed by chromatin-bound OGT through interaction with TET oxidases (TET), which have recently emerged as major epigenomic players by regulating cytosine hydroxymethylation (27). Reciprocally, OGT O-GlcNAcylates TET enzymes and alters their enzymatic properties through ill-defined mechanisms (21). We therefore tested whether REV-ERB $\alpha$  impacts on TET activity through OGT.

As described (28), glucose significantly increases TET enzymatic activity in HepG2 cells (Fig. 6A). *REV-ERB $\alpha$*  knockdown blunted Glc-induced TET enzymatic activity (Fig. 6A). *REV-ERB $\alpha$*  depletion did not reduce nuclear OGT protein content but reduced its enzymatic activity as total nuclear protein O-GlcNAcylation decreased by  $\sim$ 20% (SI Appendix, Fig. S6 A and B) without affecting TET protein levels (SI Appendix, Fig. S6C). In line, global cytosine hydroxymethylation of the HepG2 cell genome was significantly decreased upon *REV-ERB $\alpha$*  knockdown at both 1 and 25 mM Glc (Fig. 6A). GSK4112 treatment increased TET enzymatic activity at 1 mM Glc but was unable to do so at 25 mM Glc, probably reflecting a saturation of the system (SI Appendix, Fig. S6D). *REV-ERB $\alpha$*  overexpression increased cytosine hydroxymethylation, and this response were clearly blunted by OSMI-1, a cell permeable OGT inhibitor (ref. 29 and SI Appendix, Fig. S6 E and F). *REV-ERB $\alpha$*  is thus an important determinant of TET activity and controls global 5hmC levels in an OGT-dependent manner in vitro.

TET/OGT complexes are mostly targeted to promoter regions through interaction of TET with DNA (19). We thus investigated whether *REV-ERB $\alpha$*  genomic binding overlaps with 5hmC content in mouse liver. Using previously published data for C57BL/6 mouse liver (30), we confirmed that 5hmC localizes to genomic regions neighboring transcription start sites (TSS; SI Appendix, Fig. S7A). Mapping *REV-ERB $\alpha$*  genomic binding sites in C57BL/6 mouse liver (31) in the vicinity ( $\pm$ 5 kb) of TSS showed a direct correlation between *REV-ERB $\alpha$*  binding and 5hmC density (Fig. 6B and SI Appendix, Fig. S7B). 5hmC levels were measured in liver from *Rev-erba*<sup>+/+</sup> and *Rev-erba*<sup>-/-</sup> in mice (Fig. 6C). *Rev-erba*<sup>-/-</sup> mouse DNA showed a decreased 5hmC content compared with DNA from wild-type littermates while the genetic background did not affect TET protein levels (SI Appendix, Fig. S7C). Taken together, these observations show that *REV-ERB $\alpha$*  impacts on nuclear OGT activity and increases DNA 5hmC level.

In addition to nutritional regulation, *Srebp1c* expression undergoes diurnal variation, with a peak occurring at ZT14–18, which is imposed in part by *REV-ERB $\alpha$* , whose knockout decreases *Srebp1c* expression (32, 33). We first tested whether *REV-ERB $\alpha$*  regulates *SREBP1C* expression in a cell-autonomous manner. *REV-ERB $\alpha$*  deficiency in HepG2 cells decreased *SREBP1C* basal expression (Fig. 6D). *TET1*, *TET2*, or *TET3* knockdown (Fig. 6D and SI Appendix, Fig. S7D) led to a significantly decreased expression of *SREBP1C* (Fig. 6D). Thus, TETs sustain gene expression at this locus in vitro. Similarly, *Rev-erba* deficiency decreased hepatic *Srebp1c* gene expression in ad libitum-fed mice (Fig. 6E). *REV-ERB $\alpha$*  bound to genomic regions in the vicinity or within the *Srebp1* gene, and an increased 5hmC density was observed around *REV-ERB $\alpha$*  binding sites (Fig. 6F, Upper). Interestingly, 5hmC density at these sites decreased in *Rev-erba*<sup>-/-</sup> livers, thereby paralleling the decreased *Srebp1c* gene expression in this genetic background (Fig. 6F, Lower).

In conclusion, these data show that *REV-ERB $\alpha$*  controls TET oxidase activity, thereby controlling epigenomic marking at the

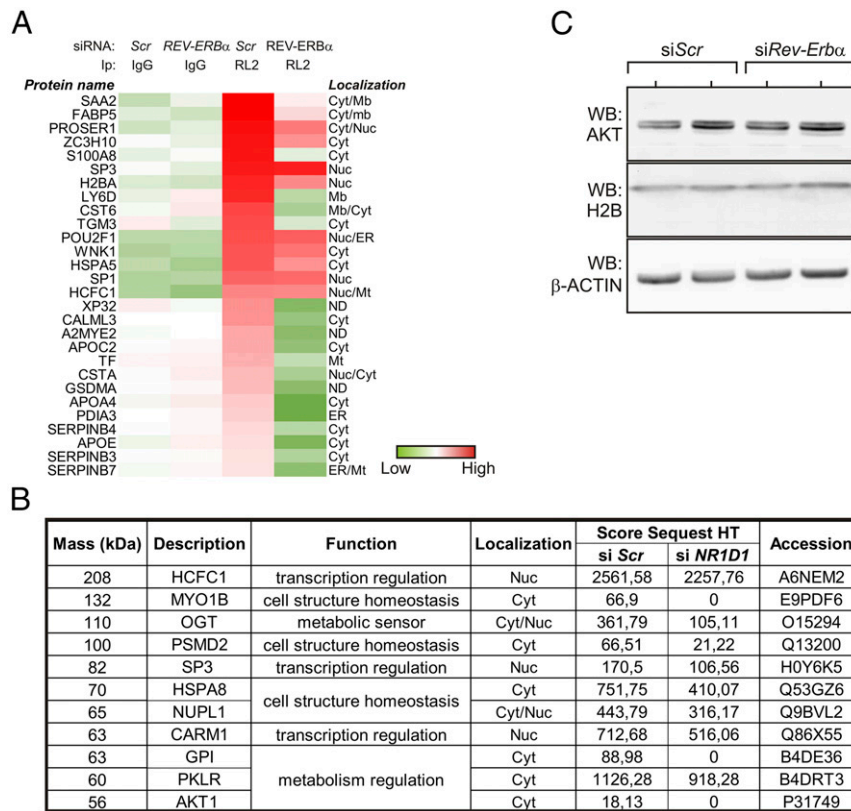


**Fig. 4.** REV-ERB $\alpha$  impacts on protein O-GlcNAcylation in both cytoplasmic and nuclear compartments. (A) Label-free mass spectrometry analysis of O-GlcNAcylated proteins. Control (IgG) or O-GlcNAcylated protein-enriched (RL2) immunoprecipitates from siRNA (Scr or REV-ERB $\alpha$ )-transfected HepG2 cells were analyzed by label-free mass spectrometry analysis. (B) LC-MS/MS analysis of O-GlcNAcylated proteins. HepG2 cells were treated like in A, and immunoprecipitates were fractionated by SDS/PAGE before mass spectrometry analysis. (C) Cellular abundance of AKT and H2B in siRNA-transfected HepG2 cells. HepG2 cells were cultured at 25 mM Glc. Cyt, cytoplasm; ER, endoplasmic reticulum; Mb, plasma membrane; Mt, mitochondria; Nuc, nucleoplasm.

*Srebfl* locus whose basal expression is regulated through the REV-ERB $\alpha$ /OGT/TET axis.

## Discussion

The regulatory pathways controlling OGT activity and expression are not yet fully understood. OGT is regulated by the UDP-GlcNAc pool, which fluctuates with the varying availability of nutrients such as glucose, glutamate, and free fatty acids. In addition, various PTMs modulate OGT activity, localization, substrate selectivity, or stability such as O-GlcNAcylation itself, phosphorylation, or ubiquitylation (2). OGT-protein partners, such as MYPT1 and CARM1, affect OGT activity or substrate selectivity (34). Reciprocally, OGT regulates the activity of numerous proteins, including circadian clock proteins (35).

In this study, we identify a mechanism regulating OGT stability and activity. We show that REV-ERB $\alpha$ , but not REV-ERB $\beta$  with which it shares only 53% amino acid sequence homology, interacts with cytoplasmic and nuclear OGT. REV-ERB $\alpha$  itself is however not a substrate for OGT, and its transcriptional properties are not affected by the HBP/OGT pathway. A synthetic REV-ERB $\alpha$  ligand favored REV-ERB $\alpha$  cytoplasmic depletion and nuclear accumulation and, consequently, induced cytoplasmic proteasomal OGT degradation, thereby compromising protein O-GlcNAcylation in this cellular compartment while increasing nuclear OGT activity. Collectively, this suggests that REV-ERB $\alpha$  unexpectedly acts as a regulator of protein stability, therefore expanding the repertoire of its biological properties beyond that of a transcriptional regulator.

Mass spectrometry analysis identified O-GlcNAcylated proteins or proteins bound to them, among which AKT was an interesting target as a key regulator of insulin signaling. AKT

phosphorylation is reduced upon OGT overexpression, hence inducing insulin resistance (36) and REV-ERB $\alpha$  (over)expression impinges on AKT phosphorylation in vitro. OGT protein level is reduced in *Rev-erba*<sup>-/-</sup> mouse liver and correlates with increased AKT phosphorylation, thus potentially impacting on hepatic insulin signaling. Interestingly, insulin signaling is a circadian-regulated phenomenon, as mice display decreased insulin signaling at ZT7 (37), corresponding to the *Rev-erba* expression zenith (Fig. 1C). In addition, AKT phosphorylation peaks at night in mouse liver when *Rev-erba* expression is lowest (38, 39). Insulin signaling follows a circadian rhythm in humans, with a low insulin responsiveness being observed in the evening when REV-ERB $\alpha$  is expressed (40, 41). These data are in line with our observation that physiologically (ZT0) or genetically induced (*Rev-erba*<sup>-/-</sup> mice) REV-ERB $\alpha$  depletion reduces liver OGT protein content and favors AKT phosphorylation, hence leading to increased insulin responsiveness. In the presence of REV-ERB $\alpha$  (ZT6–12 in mouse liver), cytoplasmic OGT is stabilized and AKT phosphorylation is decreased, hence providing a molecular basis for the observed reduced insulin signaling. Thus, circadian modulation of insulin signaling could occur, at least partly, through the REV-ERB $\alpha$ -dependent control of cytoplasmic OGT and of its target AKT.

The REV-ERB $\alpha$ /OGT interaction also occurs in the nucleus. Contrasting with cytoplasmic OGT, nuclear OGT protein level is not modulated by REV-ERB $\alpha$  expression levels. However, OGT activity is reduced upon REV-ERB $\alpha$  down-regulation, as suggested by decreased H2B O-GlcNAcylation in siRev-erb $\alpha$ -transfected HepG2 cells. The impact of nuclear REV-ERB $\alpha$  on OGT activity was investigated by monitoring TET1/2/3 oxidase

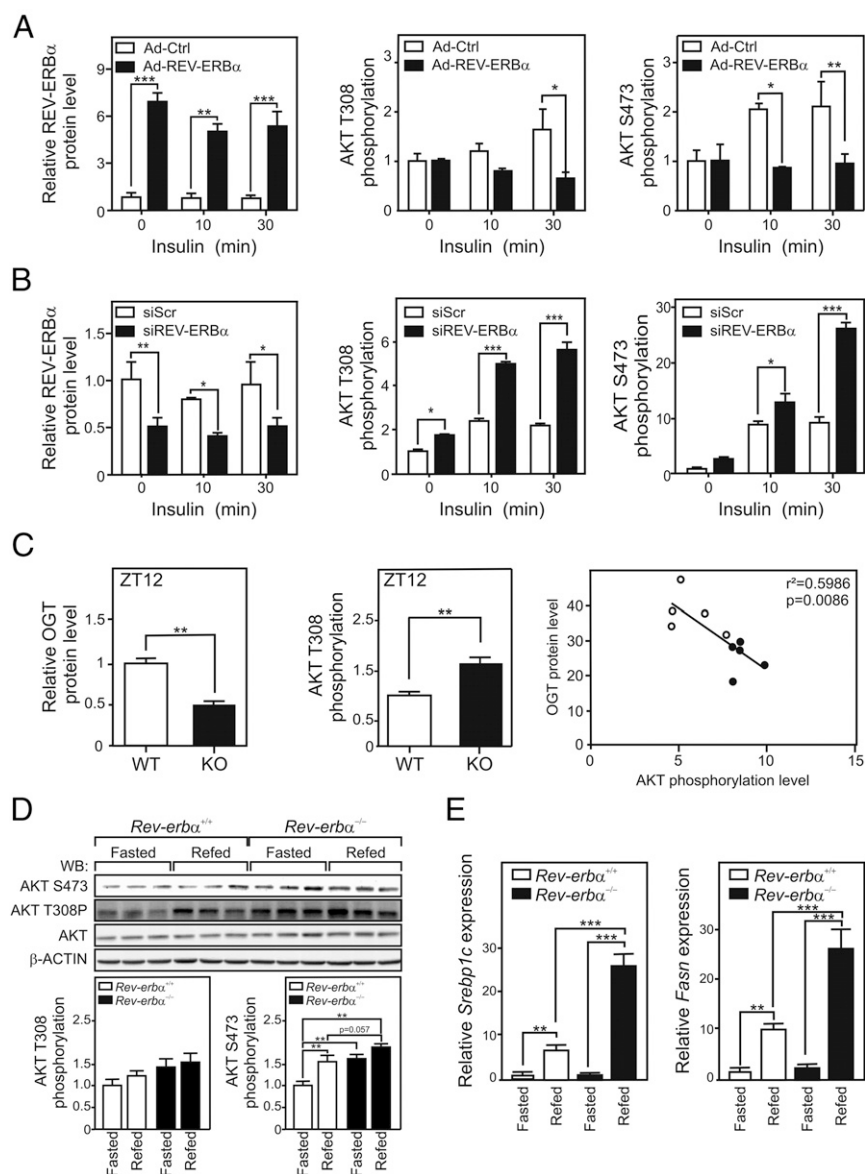


**Fig. 5.** REV-ERB $\alpha$  expression level alters AKT phosphorylation. (A) REV-ERB $\alpha$  protein level, T308, and S473 AKT phosphorylation were quantified in HepG2 cellular extracts after transduction with control (*LacZ*, open bars) or REV-ERB $\alpha$  (filled bars) adenoviruses and treated with 60 nM insulin for the indicated times. (B) HepG2 cells were transfected with siRNA (Scr and REV-ERB $\alpha$ ) and treated with 60 nM insulin for the indicated times. REV-ERB $\alpha$ , AKT T308, and S473 phosphorylation were quantified. (C) OGT (Left) and phospho-AKT T308 (Center) hepatic content. The correlation analysis in ad libitum-fed WT ( $n = 5$ ) and *Rev-erba* KO ( $n = 5$ ) mice at ZT12 (Right) was performed with data from *SI Appendix, Fig. S5E*. (D) Hepatic P-AKT T308 and AKT protein levels (ZT6) from WT or *Rev-erba* KO mice after a 30-h fast (Fasted) or refed for 6 h after fasting (Refed). (E) Relative *Srebp1c* (Left) and *Fasn* (Right) gene expression in livers (ZT6) from WT and *Rev-erba* KO mice fasted or refed as described in D. Data are expressed as mean  $\pm$  SEM. The statistical significance was assessed by a two-way ANOVA followed by a Bonferroni post hoc test (A, B, and E) or a *t* test (C). \* $P < 0.05$ , \*\* $P < 0.001$ , and \*\*\* $P < 0.001$ .

activity, which were described as glucose-sensitive and OGT-sensitive enzymes in ES cells (19, 28, 42). The REV-ERB $\alpha$ -dependant increase of TET activity and DNA hydroxymethylation are also OGT-dependent. Reduced expression of REV-ERB $\alpha$  decreases nuclear protein O-GlcNAcylation levels and blunts glucose-induced TET activity and DNA hydroxymethylation in HepG2 cells. These findings, showing that OGT contributes to increased TET activity and 5hmC content, contrast with the reported decreased protein stability of O-GlcNAcylated TET1 in ES cells (43) and increased nuclear export of O-GlcNAcylated TET3 in HeLa and HEK cells (44). It is therefore likely that TET family members, which are expressed in hepatocyte cell lines and mouse liver, are regulated in a cell/tissue-specific manner.

Comparison of the mouse liver REV-ERB $\alpha$  cistrome to the 5hmC genomic landscape (30, 31) revealed that high-density 5hmC regions localized in the vicinity of strong REV-ERB $\alpha$  DNA binding sites. Conversely, weak REV-ERB $\alpha$  binding sites associated to weakly hydroxymethylated regions, suggesting a direct relationship between REV-ERB $\alpha$  genomic binding site occupancy and DNA hydroxymethylation. No specific enrichment in HNF6-dependent or in HNF6-independent REV-ERB $\alpha$  binding sites (11, 45) was observed in our analysis. This suggested that REV-ERB $\alpha$  binding correlates with the 5hmC pattern regardless of its DNA binding mode. Furthermore, *Rev-erba* KO mice display a globally reduced liver DNA hydroxymethylation ( $\sim 35\%$ ).

Taken together, these data indicate that the REV-ERB $\alpha$ /OGT functional interaction impinges on cytosine hydroxymethylation



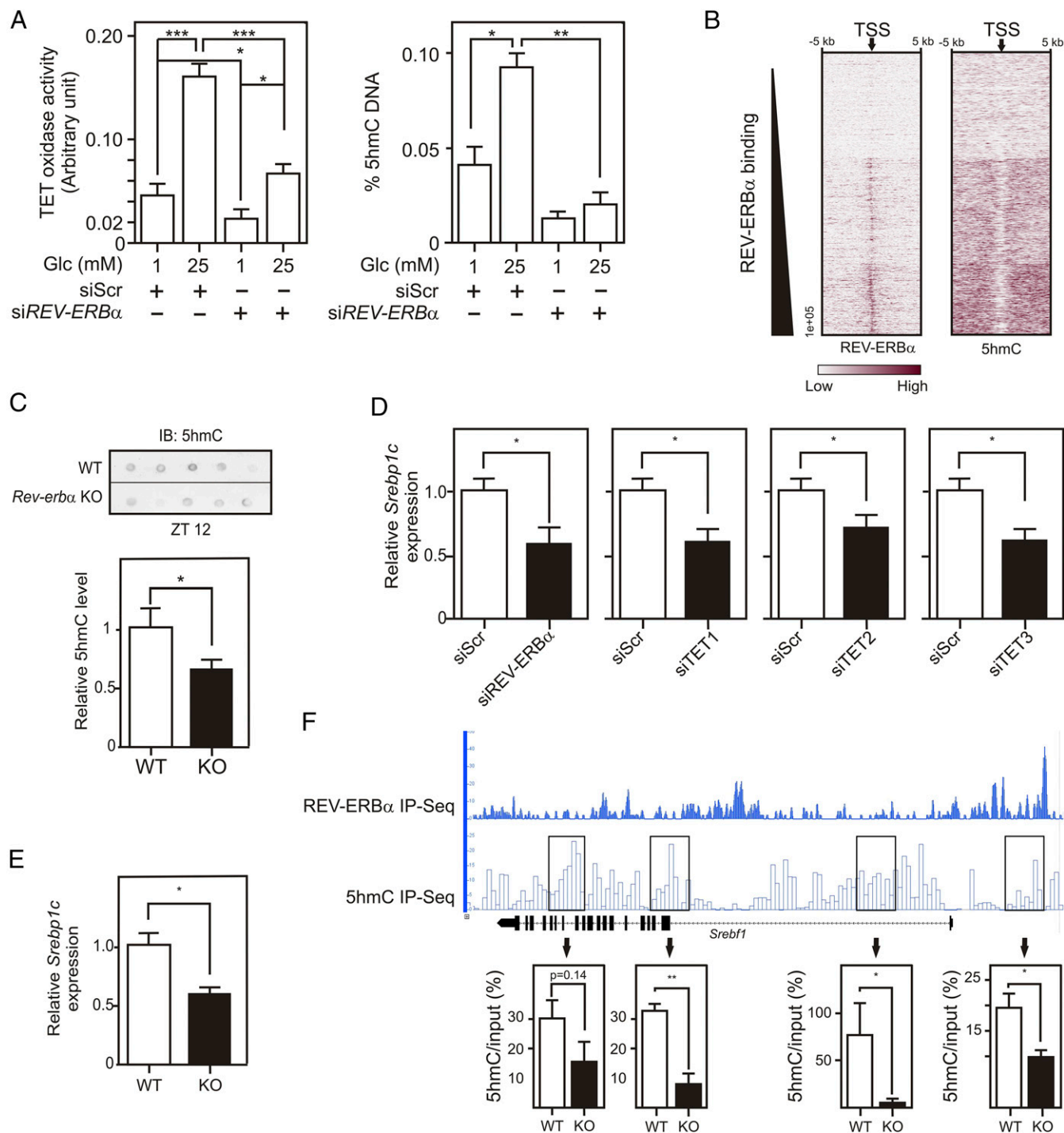


**Fig. 6.** Nuclear REV-ERB $\alpha$  controls nuclear OGT and TET activities and affects DNA hydroxymethylation. (A) TET oxidase activities (Left) and 5hmC levels (Right) in HepG2 nuclear protein extracts or in genomic DNA, respectively. Cells were transfected with siRNA (control or REV-ERB $\alpha$ ) and incubated at 1 or 25 mM Glc. (B) Heatmaps of REV-ERB $\alpha$  and 5hmC signal intensities in clustered TSS. Gencode TSS (arrow) were aligned and extended 5 kb on each side. (C) 5hmC levels in *Rev-erba*<sup>+/+</sup> (WT) and *Rev-erba*<sup>-/-</sup> (KO;  $n = 5-6$ ) mouse livers. (D) Relative *SREBP1C* gene expression determined by RT-qPCR on siRNA (Scr, REV-ERB $\alpha$ , TET1, TET2, or TET3)-transfected HepG2 cells. (E) Relative *Srebp1c* gene expression in liver from *Rev-erba*<sup>+/+</sup> or *Rev-erba*<sup>-/-</sup> mice (ZT12). (F) Representation of REV-ERB $\alpha$  chromatin occupancy and hydroxymethylated region localization at the mouse hepatic *Srebf1* locus (Upper). *Srebf1* hydroxymethylation was quantified by hMeDIP-qPCR (Bottom) in hepatic genomic DNA from *Rev-erba*<sup>+/+</sup> ( $n = 2$ ) or *Rev-erba*<sup>-/-</sup> mice ( $n = 2$ ). Histogram represents mean  $\pm$  SEM. The statistical significance of differences was assessed by a two-way ANOVA followed by a Bonferroni post hoc test (A) or by a  $t$  test. \* $P < 0.05$ , \*\* $P < 0.01$ , \*\*\* $P < 0.001$ .

both in vitro and in vivo. Predicting the transcriptional outcome of this process at the cellular level remains difficult, as several groups reported that TET1 DNA binding is not only associated with gene activation but also with gene repression (30, 46).

However, our observation that TET1/2/3 regulate *SREBP1C* expression suggests that REV-ERB $\alpha$  regulates this important lipogenic gene by altering epigenomic modifications at this locus. Since *Srebp1c* expression is not HDAC3-sensitive (47), and since

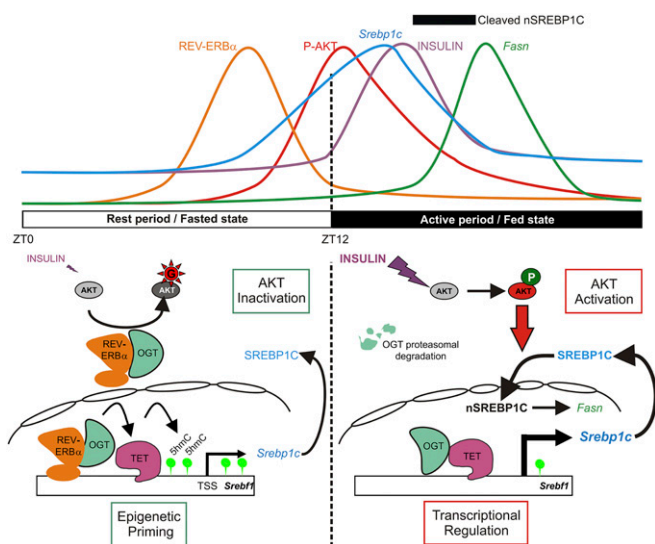


**Fig. 7.** REV-ERB $\alpha$ /OGT participates to the control of circadian metabolic flexibility. During the rest period (from ZT0 to ZT12), insulin level is low and cytoplasmic REV-ERB $\alpha$  stabilizes OGT protein, which prevents AKT phosphorylation. In the nucleus, REV-ERB $\alpha$  binds to and activates OGT, favoring TETs enzyme activity. The REV-ERB $\alpha$ -dependent TETs activation results in DNA hydroxymethylation of *Srebf1* locus enhancing *Srebp1c* basal expression. This epigenetic mechanism could prime the liver, allowing an immediate response to feeding. During the active period (from ZT12 to ZT24), the cytoplasmic OGT, which is not protected anymore by REV-ERB $\alpha$ , is degraded by the proteasome. In the nucleus, OGT and TET activities decrease in the absence of REV-ERB $\alpha$ . In parallel, insulin level increases in response to the food intake. In this context, the liver can fully respond to insulin, triggering the maturation of nSREBP1c followed by *Fasn* expression induction. Data were adapted from our and several other studies (32, 33, 38, 39).

REV-ERB $\alpha$  is not associated to HDAC3 or HNF6 at this locus (10, 11, 31), REV-ERB $\alpha$  may act as a positive regulator of *Srebp1c* expression. Whether this property actually extends beyond the control of *Srebp1c* expression awaits further investigation, but this nevertheless demonstrates that REV-ERB $\alpha$  acts as a sophisticated regulator of metabolic flexibility by interconnecting temporally and spatially hormonal signals, metabolism, and circadian rhythm. Thus, during the rest period, when insulin level is low and REV-ERB $\alpha$  is high, the REV-ERB $\alpha$ /OGT complex could act at different levels. In the cytoplasm, the REV-ERB $\alpha$ /OGT complex would block the AKT signaling pathway and, in parallel, will activate TET enzymes in the nucleus to promote an epigenomic state favoring *SREBP1C* basal expression (Fig. 7). This original REV-ERB $\alpha$ -dependant regulation could prime the liver for a faster response to insulin signaling at the start of the active phase. During the active feeding period, during which REV-ERB $\alpha$  is not expressed and when insulin peaks, cytoplasmic OGT is degraded, allowing the full activation of the AKT signaling pathway (Fig. 7). Increased DNA methylation was reported in mouse liver during the active period (48), which could result from the observed reduction of

TET activity in the absence of REV-ERB $\alpha$ . As methylation is most often a dynamic modification characterizing inactive chromatin, these reciprocal epigenomic modifications may be involved in the circadian regulation of hepatic lipogenesis.

## Experimental Procedures

**Animal Experimentation.** Animals were handled in accordance with institutional guidelines and approved by the Comité d’Ethique en Expérimentation Animale du Nord-Pas de Calais (C2EA-75). All mice (12-wk-old) were housed in a 12 h/12 h light/dark cycle for 2 wk before experimentation and fed ad libitum on a chow diet (A04, Safe Diets) with free access to drinking water. Wild-type C57BL/6J mice were from Charles River Laboratories. *Rev-erb $\alpha$*  KO and their wild-type littermates were bred at Institut Pasteur de Lille animal facility as described (49). Mice were killed by cervical dislocation, and livers were snap-frozen in liquid nitrogen and stored at  $-80^{\circ}\text{C}$  until use. Samples were thawed only once as protein O-GlcNAcylation was found to be unstable upon multiple freeze-thawing cycles.

**Chemicals.** Glucosamine, MG132, OGT inhibitors (DON and azaserine), the OGA inhibitor Thiamet G,  $\delta$ -aminolevulinic acid, and succinyl acetone were purchased from Sigma-Aldrich. Compounds were used at indicated concentrations (see figure legends).

**Cell Culture.** HepG2 cells, derived from a human hepatocellular carcinoma, were purchased from ATCC (HB8065) and grown in DMEM containing 25 mM Glc supplemented with 10% FBS, 1 mM nonessential amino acids, 1 mM sodium pyruvate, and 1% penicillin/streptomycin in a humidified incubator with 5%  $\text{CO}_2$  at  $37^{\circ}\text{C}$ . Treatments were performed as described in DMEM containing 4 mM glutamine (Life Technologies-Gibco-BRL) supplemented with 10% dextran/charcoal-treated FBS at indicated Glc concentrations. Human embryonic kidney (HEK) 293 cells were purchased from ATCC (CRL-1573) and maintained at  $37^{\circ}\text{C}$  under 5%  $\text{CO}_2$  in DMEM containing 25 mM Glc supplemented with 10% FBS and 1% penicillin/streptomycin. The U2OS cell line (HTB-96; ATCC) derived from human osteosarcoma was grown in McCoy 5A medium containing 17 mM Glc supplemented with 10% FBS and 1% penicillin/streptomycin.

The U2OS *rev-erb $\alpha$ <sup>-/-</sup>* clone was generated using the CRISPR-paired nickase technology (Sigma-Aldrich). Briefly, cells were transfected with two RNA guide-encoding vectors (pU6-gRNA HSL0002457008 and HSL0002457018) and Cas9-D10A nicking nuclease mutant encoding vector (pCMV-Cas9-D10A) using the JetPEI transfection reagent according to manufacturer recommendations. Clone selection was done by limiting dilution and screened by WB.

**Statistical Analyses.** Raw data were analyzed using GraphPad Prism 7.0. Results are expressed as mean  $\pm$  SEM ( $n = 3-6$  for in vitro experiments,  $n$  values are indicated in figure legends for in vivo experiments), and groups were compared using either a  $t$  test or ANOVA followed by a post hoc test as indicated in figure legends. Specific analyses are described in corresponding experimental procedure sections.

All other information is available in *SI Appendix*.

**ACKNOWLEDGMENTS.** This work was supported by Agence Nationale de la Recherche Grants OGlcRev and ANR-10-LABX-46, Fondation pour la Recherche Médicale Grant Equipe labellisée FRM 2015 DEQ20150331724, European Foundation for the Study of Diabetes/Lilly European Diabetes Research Program, European Commission EurhythDia FP7-health Grant 278397, and French Proteomic Infrastructure Grant ANR-10-INBS-08-03. B.S. is a recipient of Advanced European Council Grant 694717. O-GlcNAcylated protein identification was done at “Plateforme Analyses Glycoconjugués” (FR3688 FRABio, CNRS, Université de Lille).

- Levine ZG, Walker S (2016) The biochemistry of O-GlcNAc transferase: Which functions make it essential in mammalian cells? *Annu Rev Biochem* 85:631–657.
- Bond MR, Hanover JA (2013) O-GlcNAc cycling: A link between metabolism and chronic disease. *Annu Rev Nutr* 33:205–229.
- Vocadlo DJ (2012) O-GlcNAc processing enzymes: Catalytic mechanisms, substrate specificity, and enzyme regulation. *Curr Opin Chem Biol* 16:488–497.
- Guinez C, et al. (2011) O-GlcNAcylation increases ChREBP protein content and transcriptional activity in the liver. *Diabetes* 60:1399–1413.
- Ruan HB, et al. (2012) O-GlcNAc transferase/host cell factor C1 complex regulates gluconeogenesis by modulating PGC-1 $\alpha$  stability. *Cell Metab* 16:226–237.
- Lewis BA, Hanover JA (2014) O-GlcNAc and the epigenetic regulation of gene expression. *J Biol Chem* 289:34440–34448.

- Cho H, et al. (2012) Regulation of circadian behaviour and metabolism by REV-ERB- $\alpha$  and REV-ERB- $\beta$ . *Nature* 485:123–127.
- Grant D, et al. (2010) GSK4112, a small molecule chemical probe for the cell biology of the nuclear heme receptor Rev-erb $\alpha$ . *ACS Chem Biol* 5:925–932.
- Bugge A, et al. (2012) Rev-erb $\alpha$  and Rev-erb $\beta$  coordinately protect the circadian clock and normal metabolic function. *Genes Dev* 26:657–667.
- Sun Z, et al. (2013) Deacetylase-independent function of HDAC3 in transcription and metabolism requires nuclear receptor corepressor. *Mol Cell* 52:769–782.
- Zhang Y, et al. (2016) HNF6 and Rev-erb $\alpha$  integrate hepatic lipid metabolism by overlapping and distinct transcriptional mechanisms. *Genes Dev* 30:1636–1644.
- Okabe T, et al. (2016) REV-ERB $\alpha$  influences the stability and nuclear localization of the glucocorticoid receptor. *J Cell Sci* 129:4143–4154.

13. Mohammed H, et al. (2016) Rapid immunoprecipitation mass spectrometry of endogenous proteins (RIME) for analysis of chromatin complexes. *Nat Protoc* 11: 316–326.
14. Rytter SW, Tyrrell RM (2001) An HPLC method to detect heme oxygenase activity. *Curr Protoc Toxicol* Chapter 9:Unit 9.6.
15. Hering Y, et al. (2018) Development and implementation of a cell-based assay to discover agonists of the nuclear receptor REV-ERB $\alpha$ . *J Biol Methods* 5:e94.
16. Yin L, et al. (2007) Rev-erb $\alpha$ , a heme sensor that coordinates metabolic and circadian pathways. *Science* 318:1786–1789.
17. Ha C, Lim K (2015) O-GlcNAc modification of Sp3 and Sp4 transcription factors negatively regulates their transcriptional activities. *Biochem Biophys Res Commun* 467: 341–347.
18. Li T, et al. (2014) Novel role of nuclear receptor Rev-erb $\alpha$  in hepatic stellate cell activation: Potential therapeutic target for liver injury. *Hepatology* 59:2383–2396.
19. Vella P, et al. (2013) Tet proteins connect the O-linked N-acetylglucosamine transferase Ogt to chromatin in embryonic stem cells. *Mol Cell* 49:645–656.
20. Khidekel N, Ficarro SB, Peters EC, Hsieh-Wilson LC (2004) Exploring the O-GlcNAc proteome: Direct identification of O-GlcNAc-modified proteins from the brain. *Proc Natl Acad Sci USA* 101:13132–13137.
21. Dehennaut V, Leprince D, Lefebvre T (2014) O-GlcNAcylation, an epigenetic mark. Focus on the histone code, TET family proteins, and polycomb group proteins. *Front Endocrinol (Lausanne)* 5:155.
22. Ruan HB, Singh JP, Li MD, Wu J, Yang X (2013) Cracking the O-GlcNAc code in metabolism. *Trends Endocrinol Metab* 24:301–309.
23. Sarbassov DD, Guertin DA, Ali SM, Sabatini DM (2005) Phosphorylation and regulation of Akt/PKB by the rictor-mTOR complex. *Science* 307:1098–1101.
24. Yang X, Qian K (2017) Protein O-GlcNAcylation: Emerging mechanisms and functions. *Nat Rev Mol Cell Biol* 18:452–465.
25. Azzout-Marniche D, et al. (2000) Insulin effects on sterol regulatory-element-binding protein-1c (SREBP-1c) transcriptional activity in rat hepatocytes. *Biochem J* 350: 389–393.
26. Horton JD, Bashmakov Y, Shimomura I, Shimano H (1998) Regulation of sterol regulatory element binding proteins in livers of fasted and refed mice. *Proc Natl Acad Sci USA* 95:5987–5992.
27. Delatte B, Deplus R, Fuks F (2014) Playing TETris with DNA modifications. *EMBO J* 33: 1198–1211.
28. Dhaliwayo N, Sarras MP, Jr, Luczkowski E, Mason SM, Intine RV (2014) Parp inhibition prevents ten-eleven translocase enzyme activation and hyperglycemia-induced DNA demethylation. *Diabetes* 63:3069–3076.
29. Ortiz-Meoz RF, et al. (2015) A small molecule that inhibits OGT activity in cells. *ACS Chem Biol* 10:1392–1397.
30. Thomson JP, et al. (2015) DNA immunoprecipitation semiconductor sequencing (DIP-SC-seq) as a rapid method to generate genome wide epigenetic signatures. *Sci Rep* 5: 9778.
31. Feng D, et al. (2011) A circadian rhythm orchestrated by histone deacetylase 3 controls hepatic lipid metabolism. *Science* 331:1315–1319.
32. Le Martelot G, et al. (2009) REV-ERB $\alpha$  participates in circadian SREBP signaling and bile acid homeostasis. *PLoS Biol* 7:e1000181.
33. Gilardi F, et al.; CycliX Consortium (2014) Genome-wide analysis of SREBP1 activity around the clock reveals its combined dependency on nutrient and circadian signals. *PLoS Genet* 10:e1004155.
34. Cheung WD, Sakabe K, Housley MP, Dias WB, Hart GW (2008) O-linked beta-N-acetylglucosaminyltransferase substrate specificity is regulated by myosin phosphatase targeting and other interacting proteins. *J Biol Chem* 283:33935–33941.
35. Kaasik K, et al. (2013) Glucose sensor O-GlcNAcylation coordinates with phosphorylation to regulate circadian clock. *Cell Metab* 17:291–302.
36. Yang X, et al. (2008) Phosphoinositide signalling links O-GlcNAc transferase to insulin resistance. *Nature* 451:964–969.
37. Shi SQ, Ansari TS, McGuinness OP, Wasserman DH, Johnson CH (2013) Circadian disruption leads to insulin resistance and obesity. *Curr Biol* 23:372–381.
38. Robles MS, Humphrey SJ, Mann M (2017) Phosphorylation is a central mechanism for circadian control of metabolism and physiology. *Cell Metab* 25:118–127.
39. Jouffe C, et al. (2013) The circadian clock coordinates ribosome biogenesis. *PLoS Biol* 11:e1001455.
40. Carrasco-Benso MP, et al. (2016) Human adipose tissue expresses intrinsic circadian rhythm in insulin sensitivity. *FASEB J* 30:3117–3123.
41. Pinkhasov BB, Selyatinskaya VG, Astrakhantseva EL, Anufrienko EV (2016) Circadian rhythms of carbohydrate metabolism in women with different types of obesity. *Bull Exp Biol Med* 161:323–326.
42. Yang H, et al. (2014) TET-catalyzed 5-methylcytosine hydroxylation is dynamically regulated by metabolites. *Cell Res* 24:1017–1020.
43. Shi FT, et al. (2013) Ten-eleven translocation 1 (Tet1) is regulated by O-linked N-acetylglucosamine transferase (Ogt) for target gene repression in mouse embryonic stem cells. *J Biol Chem* 288:20776–20784.
44. Zhang Q, et al. (2014) Differential regulation of the ten-eleven translocation (TET) family of dioxygenases by O-linked  $\beta$ -N-acetylglucosamine transferase (OGT). *J Biol Chem* 289:5986–5996.
45. Zhang Y, et al. (2015) GENE REGULATION. Discrete functions of nuclear receptor Rev-erb $\alpha$  couple metabolism to the clock. *Science* 348:1488–1492.
46. Wu H, et al. (2011) Dual functions of Tet1 in transcriptional regulation in mouse embryonic stem cells. *Nature* 473:389–393.
47. Papazyan R, et al. (2016) Physiological suppression of lipotoxic liver damage by complementary actions of HDAC3 and SCAP/SREBP. *Cell Metab* 24:863–874.
48. Maekawa F, et al. (2012) Diurnal expression of Dnm3b mRNA in mouse liver is regulated by feeding and hepatic clockwork. *Epigenetics* 7:1046–1056.
49. Woldt E, et al. (2013) Rev-erb $\alpha$  modulates skeletal muscle oxidative capacity by regulating mitochondrial biogenesis and autophagy. *Nat Med* 19:1039–1046.